Volume 1 | Number 1 | Jan 2013 | Pages 1–100

Dalton Transactions

An international journal of inorganic chemistry
www.rsc.org/dalton

ROYAL SOCIETY OF CHEMISTRY

ROYAL SOCIETY OF CHEMISTRY

www.rsc.org/dalton

Journal Name

RSC**Publishing**

ARTICLE

Immobilization of Co-containing Polyoxometalates in MIL-101(Cr): Structural Integrity versus Chemical Transformation

William Salomon, François-Joseph Yazigi, Catherine Roch-Marchal,[*] Pierre Mialane, Patricia Horcajada, Christian Serre, Mohamed Haouas, Francis Taulelle and Anne Dolbecq[*]

The encapsulation of three different cobalt substituted polyoxometalates (POMs) within the mesoporous chromium(III) terephthalate MIL-101(Cr) metal-organic framework (MOF) was studied by a simple and green impregnation method using water. The POM@MIL composite materials were fully characterized by EDX, XRPD, IR, MAS NMR and N_2 porosimetry measurements. The encapsulated POMs were then extracted by an exchange procedure using LiCl solution. ^{31}P NMR spectroscopy is the key experiment which indicates that the monosubstitued Keggin anion $[PW_{11}CoO_{39}(H_2O)]^{5-}$ (PW$_{11}$Co) and the sandwich-type anion $[(PW_9O_{34})_2Co_4(H_2O)_2]^{10-}$ (P$_2$W$_{18}$Co$_4$) can be encapsulated and extracted without degradation, neither of the POM nor of the MOF, while the hybrid sandwich-type POM $[(PW_9O_{34})_2Co_7(OH)_2(H_2O)_4(O_3PC(O)(C_3H_6NH_3)PO_3)_2]^{14-}$ (Co$_7$-Ale) evolves into P$_2$W$_{18}$Co$_4$ inside the cavities of the mesoporous material. The PW$_{11}$Co Keggin anion is the most quantitatively uploaded and the most easily extracted anion. ^{31}P MAS-NMR spectroscopy further suggests that this anion is more mobile inside the cavities of the MOF than the P$_2$W$_{18}$Co$_4$ POM.

Introduction

Polyoxometalates (POMs) constitute a large family of soluble anionic metal oxide clusters of *d*-block transition metals in high oxidation states (W^{VI}, $Mo^{V,VI}$, $V^{IV,V}$), with a wide range of magnetic,[1] redox,[2] and catalytic properties.[3] Most of the applications require the design of materials where the POMs are immobilized on supports. One specific aim is to obtain stable heterogeneous catalysts with high surface areas, which could combine the activity of the POMs with the advantages of heterogeneous catalysts, such as an easier recovery and recycling. For example, POMs have been anchored to silica surfaces,[4] titania,[5] or active carbon.[6] Encapsulation of POMs within the cavities of metal organic frameworks (MOFs)[7] has also attracted a lot of interest for a few years.[8] Indeed, MOFs, tuneable crystalline solids built up from inorganic units and poly-complexing linkers, present a versatile and highly micro- or meso-porous architecture with important surface area and cavities large enough to allow the diffusion of molecules, even after the encapsulation of POMs. Furthermore, they can be considered as non-innocent supports as they can bring themselves additional properties to the POMs and lead eventually to synergistic effects. Three families of MOFs have been mainly studied as host matrices.[8] The first one, a microporous Cu-BTC framework (BTC = 1,3,5-benzene-tricarboxylate), known as HKUST-1 (HKUST stands for Hong-

Kong University of Science and Technology), offers the advantage of allowing single crystal X-ray diffraction characterization. However, due to the relatively small size of the cavities, only monomeric Keggin-type POMs can be incorporated.[9] In addition, these Cu-MOFs exhibit a rather limited hydrolytic stability.[10] In these compounds, it has been shown that the Keggin POM exhibits a templating effect during the formation of the MOF.[11] Beside this Cu-BTC MOF, the mesoporous metal(III)-trimesate MIL-100 and -terephthalate MIL-101 families (MIL stands for Material of Institut Lavoisier) have been widely investigated (M=Fe, Cr…). Although these MOFs exhibit cavities far larger than those of Cu-BTC, the reported works deal quasi exclusively with the encapsulation of monomeric Keggin-type POMs either by impregnation[12] or *in situ* during the MOF synthesis.[13] The encapsulation of peroxotungstate complexes $[XW_4O_{24}]^{3-}$ (X = P, B)[12b,14] constitutes one example of non monomeric Keggin POMs. Very recently, the immobilization of lanthanopolyoxometalates, $[Ln(PW_{11}O_{39})_2]^{11-}$ (Ln = Eu^{3+}, Sm^{3+}),[15] and of $[(PW_9O_{34})_2Co_4(H_2O)_2]^{10-}$ (P$_2$W$_{18}$Co$_4$)[16] have been also performed in the mesoporous chromium(III)-terephtalate MIL-101(Cr).

Following our previous work on the incorporation of $[PMo_{12}O_{40}]^{3-}$ in the mesoporous iron(III) trimesate MIL-100(Fe) by direct synthesis,[13b] we have initiated a study on the encapsulation of sandwich-type POMs, starting with two Co-containing

polyoxotungstates. The first one is $P_2W_{18}Co_4$ built up from two trivacant $[PW_9O_{34}]^{10-}$ units, which sandwich a rhombic tetranuclear Co^{II} cluster (Fig. 1a). Among the family of transition metal-substituted polyoxotungstates, $P_2W_{18}Co_4$ is one of the most studied, because of its magnetic[17] and catalytic[4c] properties. Especially, catalytic water oxidation has attracted recently a lot of interest.[18] Although $P_2W_{18}Co_4$ was previously entrapped within the MIL-101 solid,[16] we here propose a greener procedure based on water (*vs.* CH_3CN) which is related to a different nature of the counter-ions (potassium versus tetrabutylammonium).

While $P_2W_{18}Co_4$ is a fully inorganic species, the second POM precursor involved in this study, $[(PW_9O_{34})_2Co_7(OH)_2(H_2O)_4(O_3PC(O)(C_3H_6NH_3)PO_3)_2]^{14-}$ (Co$_7$-Ale, Ale = alendronate; Fig. 1b and c) represents a rare example of a hybrid organic inorganic 3d- substituted sandwich type POM.[19] Co$_7$-Ale is built of a heptanuclear Co^{II} core sandwiched by two $[PW_9O_{34}]^{10-}$ units and connected to two bisphosphonate ligands (alendronate ligands, Fig. 1c) each one possessing a terminal ammonium group. Its stability in aqueous solution, even at high temperature, has been demonstrated by various techniques.[19] Finally, the encapsulation of the Co-monosubstituted Keggin anion $[PW_{11}CoO_{39}(H_2O)]^{5-}$ (PW$_{11}$Co, Fig. 1d) has also been studied as a reference in order to evaluate the influence of the size, charge and shape of the POM on the insertion. The encapsulation of this POM had been previously studied by Kholdeeva et al. for catalytic purposes but again the impregnation reactions were performed in CH_3CN using the tetrabutylammonium salt of the POM.[12a]

These three Co-substituted POMs offer the advantage of exhibiting well-defined UV-vis spectra and P atoms presenting characteristic nuclear magnetic resonances. We chose as support the highly chemically and thermally stable MIL-101(Cr) (Fig. 1e), built up from chromium(III) octahedral trimers and terephthalate anions, which creates a 3D cubic zeotype structure with two types of mesocages ($\varnothing$ = 29 and 34 Å) accessible through microporous windows ($\varnothing$ = 11 and 16 Å). The largest cages, accessible via hexagonal windows (16 Å) should be sufficiently large to allow the diffusion and incorporation of the $P_2W_{18}Co_4$ (~12 x 12 x 16 Å^3) and Co$_7$-Ale (~12 x 12 x 23 Å^3) POMs. This assumption was also supported by a study performed in our group showing the successful incorporation in MIL-101(Cr) of the Dawson-type anion $[P_2Mo_{18}O_{62}]^{6-}$,[20] which possesses dimension and charge close to the sandwich-type POM $P_2W_{18}Co_4$.

We thus report here the synthesis of the composite materials PW$_{11}$Co@MIL, $P_2W_{18}Co_4$@MIL and PWCo@MIL obtained by aqueous impregnation of MIL-101(Cr) with PW$_{11}$Co, $P_2W_{18}Co_4$ and Co$_7$-Ale, respectively. The notation PWCo@MIL was adopted instead of Co$_7$-Ale@MIL as it has been shown that the Co$_7$-Ale POM precursor evolves inside the MOF. A large panel of characterizations have been used to study the nature of the POMs in the composite materials.

Experimental section

Chemical and reagents. The synthesis of MIL-101(Cr) was adapted from the protocol first described by Férey et al.[21] The MOF was synthesized in the absence of HF, as described also by Hatton et al.[12d] $Cs_5[PW_{11}O_{39}Co(H_2O)]\cdot8H_2O$ (Cs$_5$PW$_{11}$Co),[22] $K_{10}[(PW_9O_{34})_2Co_4(H_2O)_2]\cdot20H_2O$ (K$_{10}$P$_2$W$_{18}$Co$_4$)[23] and $Na_9(NH_4)_5[(PW_9O_{34})_2Co_7(OH)_2(H_2O)_4(O_3PC(O)(C_3H_6NH_3)PO_3)_2]\cdot35H_2O$ (Na$_9$(NH$_4$)$_5$(Co$_7$-Ale))[19] have been synthesized according to reported procedures. $P_2W_{18}Co_4$ was recrystallized twice before use. All other chemicals were used as purchased without purification.

Synthesis of POM@MIL composite materials (Fig. 2). For the synthesis of PW$_{11}$Co@MIL, Cs$_5$PW$_{11}$Co (0.400 g, 1.12 10^{-4} mol) was dissolved in 20 mL of water. MIL-101(Cr) (0.250 g, 3.20 10^{-4} mol) was added and the solution was stirred for 24 h at room temperature. The pH was measured before (6.1) and after the impregnation experiment and the removal of MIL-101(Cr) (4.7). The suspension was centrifuged (15000 rounds per min during 15 min) and the solid washed three times with water and dried with EtOH and Et$_2$O and then placed in an oven at 393 K during 24 h. Anal. calcd (found) for $[Cr_3(H_2O)_3O(O_2CC_6H_4CO_2)_3][PW_{11}O_{39}Co(H_2O)]_{0.2}\cdot2EtOH$: C 24.70 (24.96), H 2.25 (2.15), Co 0.86 (0.59), Cr 11.46 (10.36). N was only detected as traces.

The same protocol was used for the synthesis of $P_2W_{18}Co_4$@MIL, starting with K$_{10}$P$_2$W$_{18}$Co$_4$ (0.350 g, 6.34 10^{-5} mol) and MIL-101(Cr) (0.219 g, 2.80 10^{-4} mol) in 17.5 mL of water. Anal. calcd. (found) for $[Cr_3(H_2O)_3O(O_2CC_6H_4CO_2)_3][P_2W_{18}O_{68}Co_4(H_2O)_2]_{0.1}$: C 24.19 (24.66), H 1.56 (1.93), Co 1.98 (2.25), Cr 13.09 (13.59). N was only
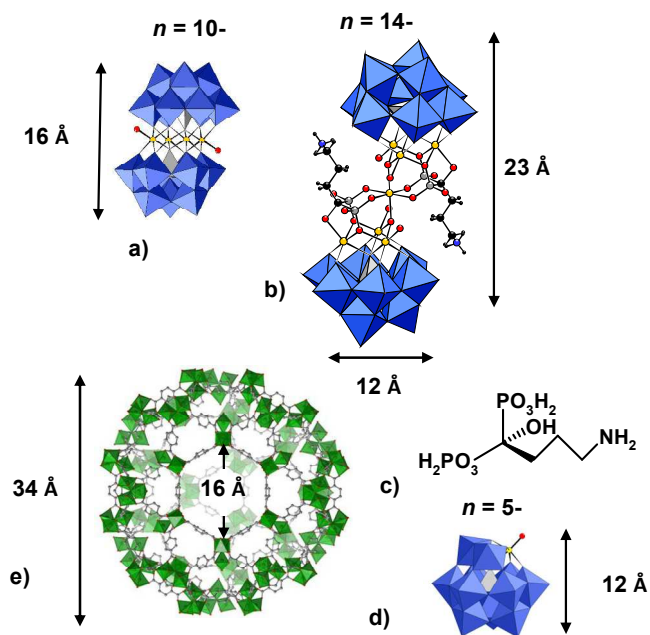

Fig. 1. Mixed ball and stick and polyhedral representation with charge and approximate dimensions of a) $[(PW_9O_{34})_2Co_4(H_2O)_2]^{10-}$ (P$_2$W$_{18}$Co$_4$), b) $[(PW_9O_{34})_2Co_7(OH)_2(H_2O)_4(O_3PC(O)(C_3H_6NH_3)PO_3)_2]^{14-}$ (Co$_7$-Ale), c) formula of the alendronic acid, d) $[PW_{11}CoO_{39}(H_2O)]^{5-}$ (PW$_{11}$Co) and e) representation of the largest cages of MIL-101(Cr); blue octahedra: WO$_6$, grey tetrahedra: PO$_4$, green octahedra: CrO$_6$, yellow spheres : Co, red spheres: O, black spheres: C, grey spheres: P, blue spheres : N, small black spheres : H.

detected as traces. The pH was measured before (6.7), and after the impregnation experiment and the removal of MIL-101(Cr) (5.1).

PWCo@MIL was synthesized following the same protocol, starting with $Na_9(NH_4)_5(Co_7-Ale)$ (0.246 g, 3.84 10^{-5} mol) in 15 mL of water to which MIL-101(Cr) (0.200 g, 2.56 10^{-4} mol) was added. The pH was measured before (6.8), and after the impregnation experiment and the removal of MIL-101(Cr) (6.0).
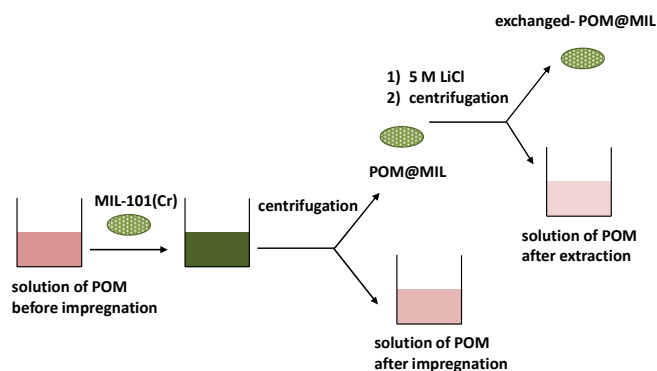

Fig. 2. Scheme summarizing the various steps for the synthesis of the POM@MIL materials and the extraction of the POM.

Extraction of the POM from the POM@MIL materials (Fig. 2). In a typical experiment a suspension of POM@MIL (0.250 g) in 10 mL of 5 M LiCl was stirred for 24 h at room temperature. The solid was collected after centrifugation, washed with H_2O, EtOH and Et_2O and dried in an oven at 393 K during 24 h.

Physical methods. Infrared (IR) spectra were recorded on a Nicolet 30 ATR 6700 FT spectrometer. Powder diffraction data was obtained on a Bruker D5000 diffractometer using Cu radiation (1.54059 Å). Electronic absorption spectra were recorded on a Perkin-Elmer Lambda 19 spectrometer. The solutions containing solid phases were centrifuged before the spectrum was recorded. EDX measurements were performed on a JEOL JSM 5800LV apparatus. N_2 adsorption isotherms were obtained at 77 K using a BELsorp Mini (Bel, Japan). Prior to the analysis, approximately 30 mg of sample were evacuated at 70°C under primary vacuum overnight.

NMR spectroscopy. The ^{31}P NMR solution spectra were recorded in 5 mm o.d. tubes with a Bruker Avance II 400 spectrometer equipped with a BBI probehead and operated at a magnetic field strength of 9.4 T. D_2O was used as solvent. ^{31}P MAS NMR spectra were obtained on a Bruker ADVANCE 500 spectrometer at 202.5 MHz with spinning rate of 21 kHz. Chemical shifts are referenced to external 85% H_3PO_4.

Results and Discussion

Synthesis. The POM@MIL-101(Cr) materials were synthesized by an impregnation method, following a procedure first described by Férey et al.[21] and which has now been used by several groups.[12] This method is based on the anionic exchange between the counter-ions of the MOF (eg. F^-, Cl^-, NO_3^-…) and the negatively charged POMs

(see experimental section). As here the synthesis of MIL-101(Cr) has been performed in the absence of HF, the counter-ions are nitrate ions coming from the $Cr(NO_3)_3$ precursor used in the hydrothermal synthesis (see experimental section). Elemental analysis indicates that the formula of MIL-101(Cr) after purification can be written as $[Cr^{III}_3(H_2O)_3O(O_2CC_6H_4CO_2)_3]NO_3\cdot2EtOH$. Considering the formula of MIL-101(Cr), the maximum number of POMs that can be loaded depends on their charge n and is equal to 1 POM for n formula units of MIL-101(Cr). The impregnation experiments were performed with a large excess of POMs (MIL-101(Cr):POM ratio ≈ 3, 4 and 6.5 for $PW_{11}Co$, $P_2W_{18}Co_4$ and Co_7-Ale, respectively, compared to the ratio deduced from a charge compensation calculation: 5, 10 and 14, respectively). The immobilization of the POMs was thus carried out by suspending the MIL-101(Cr) solid in an aqueous solution of the POM for 24 h (Fig. 2). After impregnation, the composite materials were carefully washed with water, until colourless solution, and ethanol and dried.

Characterizations of the composite materials.

IR spectra. The comparison of the FT-IR spectra of MIL-101(Cr), the POM@MIL materials and the POM precursors (Fig. 3) confirms that composite materials have been synthesized. Indeed the IR spectra can be seen as the superimposition of the IR spectrum of the MIL-101(Cr) MOF, which is only slightly affected by the presence of the POM, and vibrations typical of POM frameworks. In particular the presence of $\nu_{as}(P-O)$ and $\nu_{as}(W=O)$ vibrational bands in the 1090-1030 and 980-900 cm^{-1} regions respectively is clearly visible in the IR spectrum of the three materials
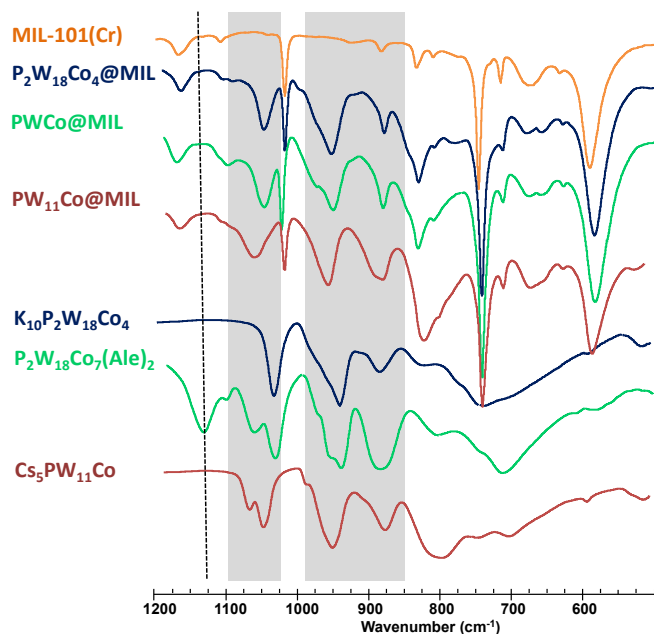

Fig. 3. Infrared spectra of the POM@MIL materials compared to that of the precursors. The regions with characteristic peaks of the POMs (P-O, W=O and W-O-W vibrations) are highlighted in grey. The dashed line indicates the position of the P-O vibration of the bisphosphonate group in Ale.

For $PW_{11}Co$@MIL and $P_2W_{18}Co_4$@MIL, the bands of the POM precursors are slightly modified. For example, the P-O vibration

which is split for $PW_{11}Co$ in two bands at 1052 and 1074 cm^{-1} merges into a single band at 1059 cm^{-1} in $PW_{11}Co@MIL$ while this P-O vibration is shifted from 1030 to 1048 cm^{-1} from $P_2W_{18}Co_4$ to $P_2W_{18}Co_4@MIL$. Such a shift is not surprising and has been previously observed in the $H_3PMo_{12}@MIL-100(Fe)$[13b] and $H_3PW_{12}O_{40}@MIL-100(Cr)$[13d] composites, being attributed to the POM-MIL interactions. The situation is different for $PWCo@MIL$ where the vibration bands of the Co_7-Ale precursor cannot be clearly identified. More specifically, the P-O vibration at 1117 cm^{-1}, attributed to the P-O groups of the bisphosphonate ligand observed in Co_7-Ale, is absent in the composite material (Fig. 3). In addition, the great similitude between the IR spectra of $P_2W_{18}Co_4@MIL$ and $PWCo@MIL$ materials can be underlined.

X-ray powder diffraction and porosimetry experiments. The positions of the Bragg reflections are similar in the X-ray powder diffraction (XRPD) pattern of MIL-101(Cr) and of the POM@MIL materials confirming the stability of the MOF structure (Fig. S1). The variation of the intensity of the peaks at low angle might be due to a significant change in the electronic density within the pores of MIL-101(Cr), in agreement with the encapsulation of the POM within the pores.[13b] In this sense, for the three POM@MIL compounds the surface area (S_{BET}) decreases as well as the total pore volumes which indicates that the POMs are located within the cavities of the MOF leaving however some residual porosity accessible to nitrogen (see Fig. 4, Fig. S2 and Table S1). Modifications of the pore size distributions also confirm the filling of the cavities with a significant shift to lower diameter and decreases of dVp/ddp (Fig. S3).
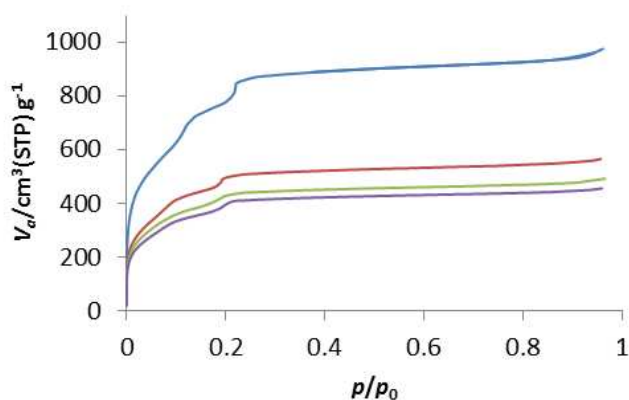

Fig. 4. N_2 adsorption/desorption isotherm (77K, P/P_0=1 atm.) of MIL-101(Cr) (blue), $PW_{11}Co@MIL$ (red), $P_2W_{18}Co_4@MIL$ (green) and $PWCo@MIL$ (purple).

UV-vis spectra of the POM solutions, EDX measurements and elemental analysis. The immobilization of the POMs was monitored by UV-vis spectroscopy. The UV-vis spectra of the aqueous solution of the POM before and after impregnation were compared. These results are shown in Fig. 5 for the experiment with $P_2W_{18}Co_4$ and in Fig. S4 and S5 for $PW_{11}Co$ and Co_7-Ale. For $P_2W_{18}Co_4$ and $PW_{11}Co$, the overall shape of the absorbance spectrum is maintained, with a lower intensity, as can be expected due to the immobilization of the POM. The amount of POM, which

has been encapsulated during the impregnation experiment with $P_2W_{18}Co_4$, can be estimated by comparing the absorbances at $\lambda =$ 574 nm before and after impregnation (Figure S4). These values are consistent with the results deduced from EDX (Table S1) and elemental analysis measurements and allow to propose the formula $[Cr_3(H_2O)_3O(O_2CC_6H_4CO_2)_3][P_2W_{18}O_{68}Co_4(H_2O)_2]_{0.1}$ (W/Cr = 0.60) and $[Cr_3(H_2O)_3O(O_2CC_6H_4CO_2)_3][PW_{11}O_{39}Co(H_2O)]_{0.2}$ (W/Cr = 0.73) for the composite material $P_2W_{18}Co_4@MIL$ and $PW_{11}Co@MIL$ respectively.

These quantitative results fit remarkably well with the expected theoretical maximum number of POMs *per* MOF that could be encapsulated on the basis of charge balance (see above). They suggest that in $PW_{11}Co@MIL$, an average of 6.8 $PW_{11}Co$ POMs occupy the largest cavities while only 3.4 $P_2W_{18}Co_4$ POMs *per* large cage are present in $P_2W_{18}Co_4@MIL$ (considering that the small cavities are not occupied). This model is usually admitted with the exception of large POM payload in a $PW_{12}O_{40}@MIL-101(Cr)$ composite.[12d]
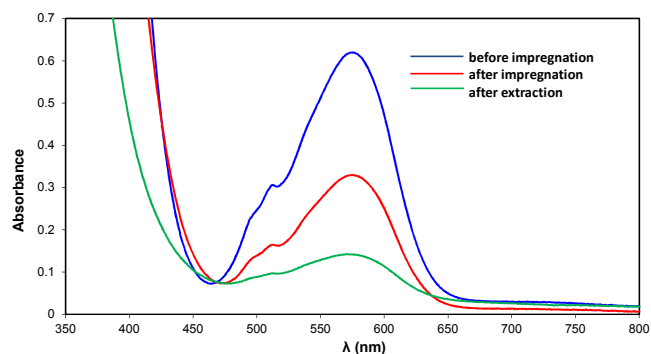

Fig. 5. UV-vis spectra of a solution of $P_2W_{18}Co_4$ (3.6 10^{-3} mol.L^{-1}), the same solution 24 h after addition of MIL-101(Cr) and the solution obtained by exchange of $P_2W_{18}Co_4@MIL$ with LiCl.

The situation is more complex for Co_7-Ale. Indeed, the comparison of the UV-vis spectra of the solutions of Co_7-Ale before and after impregnation shows that Co_7-Ale is present in solution after impregnation but together with other unidentified species with an intense absorption band below 450 nm (Fig. S5). This is in agreement with the appearance of a yellowish colour of the solution after impregnation. Furthermore, the comparison of the IR spectrum (see above) and EDX analyses with the results observed for $P_2W_{18}Co_4@MIL$ suggest that the encapsulated POM is not Co_7-Ale but $P_2W_{18}Co_4$. It should be noted also that the W/P ratio is far lower than the expected one for a pure $P_2W_{18}Co_4@MIL$ composite, which is in favour of the presence of alendronate ligands inside the nanocages together with the POM. However, it is quite difficult to propose a precise formula for this composite material.

^{31}P NMR experiments. Each POM precursor possesses P atoms with clearly distinct resonances, giving rise to a specific signature of the POM. ^{31}P NMR experiments have thus been performed for the identification of POMs not only in the solutions but also in the solid state. $PW_{11}Co$ anion is characterized by a resonance at *ca*. 465 ppm in D_2O solution (Fig. S6a). The

comparison of the ^{31}P NMR spectra of the PW$_{11}$Co solution before and after impregnation indicates the stability of the POM in the solution after impregnation (Fig. S6b). ^{31}P MAS NMR spectrum of PW$_{11}$Co@MIL (Fig. 6) further confirms the integrity of the mono-substituted POM inside the MIL. Indeed a sharp resonance at *ca.* 415 ppm is observed. The observed up-field shift of *ca.* 50 ppm compared to the liquid state indicates a shielding effect, which may be due to a confined environment.
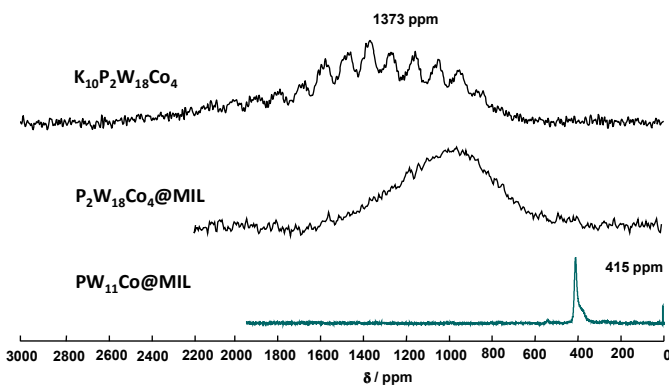

Fig. 6. ^{31}P NMR spectra of K$_{10}$P$_2$W$_{18}$Co$_4$, P$_2$W$_{18}$Co$_4$@MIL and PW$_{11}$Co@MIL under MAS. The broad spectra of P$_2$W$_{18}$Co$_4$@MIL and K$_{10}$P$_2$W$_{18}$Co$_4$ were presented in magnitude-mode after Fourier Transform.

The sandwich-type anion P$_2$W$_{18}$Co$_4$ is characterized in solution by a resonance at *ca.* 1866 ppm (Fig. 7) as also shown by other groups[18e] and in the solid state by a large peak at *ca.* 1373 ppm (Fig. 6). The presence of a single peak at 1869 ppm in the solution after impregnation shows the absence of evolution of the POM. ^{31}P MAS NMR spectrum was less conclusive than for PW$_{11}$Co@MIL (Fig. 6) as the presence of a very broad signal was observed probably due to paramagnetic interactions with the chromium centre of the MOF framework and/or severe restricted dynamic mobility within the cavity. The confinement effect on P$_2$W$_{18}$Co$_4$ should be higher than on the smaller POM PW$_{11}$Co. The broadness of the ^{31}P NMR spectrum of P$_2$W$_{18}$Co$_4$@MIL under MAS may indicate that P$_2$W$_{18}$Co$_4$ POMs are strongly anchored to the MIL framework while the PW$_{11}$Co POMs are more mobile as shown by the ^{31}P NMR spectrum of PW$_{11}$Co@MIL under MAS, averaging out to zero any anisotropic interaction including g-tensor. The fact that the Keggin type POM PW$_{11}$Co possesses some degree of mobility within the cavities of the MOF is in agreement with the observation made by Paes de Sousa *et al.* who observed that the redox processes of the monovacant [PW$_{11}$O$_{39}$]$^{7-}$ and [SiW$_{11}$O$_{39}$]$^{8-}$ POMs are diffusion-controlled instead of surface-controlled as could be expected once encapsulated in MIL-101(Cr).[25]

Finally, the ^{31}P NMR spectrum of a solution of Co$_7$-Ale before and after impregnation (Fig. 7) presents two resonances at *ca.* δ = 1700 and 1400 ppm with an integration ratio of 2:1, which are characteristic of the Co$_7$-Ale precursor.[17] The resonance located downfield corresponds to the phosphorous atoms of the coordinated bisphosphonato ligands while the upfield signal is attributed to the phosphorous atoms of the {PW$_9$} fragments. This indicates the

stability of the Co$_7$-Ale POM in solution during the impregnation experiment. For both the PWCo@MIL and the P$_2$W$_{18}$Co$_4$@MIL, the key experiment to determine the nature of the encapsulated POM has been the recording of the ^{31}P NMR solutions after extraction of the POM (see below).

Extraction of the POM. With the aim to identify the encapsulated species in solution (by UV-vis and ^{31}P NMR spectroscopy), we have attempted to extract the POMs immobilized in the composite material using an ionic exchange. When the POM@MIL solids are dispersed in a 5 M NaNO$_3$ solution, no colour change of the solution is observed while in 5 M LiCl (Fig. 2) a pink coloration progressively appears, tentatively attributed to the POM anions exchanged by Cl$^-$. The colour is more pronounced for PW$_{11}$Co@MIL than for the two other composite materials. This confirms that the interaction between the encapsulated POM and the MIL is electrostatic, as previously suggested by IR and MAS NMR and indicates that chloride and POM anions have more affinity than nitrate ions for the MIL. Noteworthy that such extraction reaction has been only rarely studied.[12a,f]
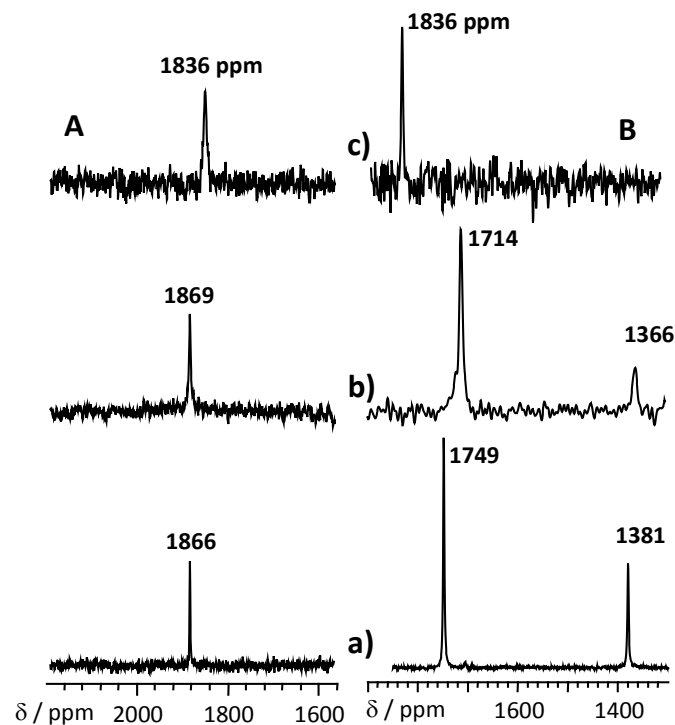

Fig. 7. ^{31}P NMR spectra of a solution of A) P$_2$W$_{18}$Co$_4$ and B) Co$_7$-Ale a) before impregnation, b) after impregnation, and c) after extraction.

After extraction, UV-vis (Fig. S4) and EDX analyses (Table S2) indicate that PW$_{11}$Co can be quantitatively exchanged from the MOF while P$_2$W$_{18}$Co$_4$ can only be partially extracted in P$_2$W$_{18}$Co$_4$@MIL. Indeed EDX measurements (Table S2) indicate that only 20% of the P$_2$W$_{18}$Co$_4$ can be extracted from the MIL-101(Cr), which is confirmed by the value deduced from the absorbance measured at 574 nm on the UV-vis spectrum of the solution after extraction (Fig. S4). Comparison of the ^{31}P NMR spectra of the solution after extraction and before impregnation (Fig. 7) clearly indicates that the

integrity of the POM is maintained in the $P_2W_{18}Co_4@MIL$ composite material. The difference in chemical shift (1836 vs 1866 ppm) can be explained by the difference of counter-ions (lithium vs potassium) and of ionic strength (water vs 5M LiCl) of the studied solutions. Furthermore, EDX measurements (Table S2) confirm the presence of Cl⁻ anions, which replace the negatively charged POM species.

After exchange of the immobilized POMs with LiCl, XRPD of the exchanged-$P_2W_{18}Co_4@MIL$ and -PWCo@MIL do not show any striking difference with the composite MIL materials (Fig. S1) while the exchanged-$PW_{11}Co@MIL$ shows a very close XRPD pattern to that of MIL-101(Cr) before impregnation. This confirms that only the $PW_{11}Co@MIL$ material can be quantitatively exchanged with chloride anions. In agreement to this last, nitrogen isotherms and pore size distributions of exchanged-$PW_{11}Co@MIL$ are very close to those of bare MIL-101(Cr) (Fig. S2), confirming once again that almost all the POMs can be extracted from the MOF. Similarly, after POM extraction in $PW_{11}Co@MIL$, the P-O and W-O bands characteristic of the encapsulated POM have almost disappeared (Fig. S8), indicating a successful exchange of the POM. On the contrary, only a weak diminution of the intensity of the POM vibrations is observed for the exchanged-$P_2W_{18}Co_4@MIL$ and -PWCo@MIL.

Finally, concerning solution after extraction of the POM from the PWCo@MIL, the expected ³¹P NMR peaks of the Co₇-Ale POM are absent and instead, a single peak at *ca*. 1836 ppm is observed (Fig. 7). This peak can be unambiguously attributed to $P_2W_{18}Co_4$ sandwich-type POMs when compared to the signal observed in solution after extraction of $P_2W_{18}Co_4$ from $P_2W_{18}Co_4@MIL$ (Fig. 7).

The occurrence of the signal at 1836 ppm after extraction and its absence in the solution after impregnation clearly indicates the conversion of Co₇-Ale anions into $P_2W_{18}Co_4$ anions inside the MOF after the encapsulation of the POMs. No free $P_2W_{18}Co_4$ anions and no free bisphosphonate ligands have been detected in solution after impregnation of Co₇-Ale. The cavities of the MOF material thus act as nanoreactors inducing the transformation of the hybrid sandwich-type POMs. EDX measurements suggest the presence of alendronate ligands into the MOF. Two explanations can be proposed to account for the instability of the hybrid Co-containing POM under the impregnation conditions. The first one is the presence of Brönsted acid sites inside the MOF which have been evidenced in the related MIL-100(Cr) and results from terminal water molecules polarized by the chromium ions.[25] The second one relies on the observations made by several authors concerning the influence of the counter-ions on the stability of POMs, and especially sandwich-type species.[18b] Contant and Hervé have also discussed the influence of the nature of the alkali cations on the formation, stability and reactivity of polyoxotungstates.[26] As Co₇-Ale anions lose their sodium and tetramethylammonium counter-ions when they are encapsulated in MIL-101(Cr), this can affect their stability.

Conclusions

In conclusion, the immobilization of three types of Co-substituted POMs in the mesoporous MIL-101(Cr) has been carried out by a green impregnation method. FT-IR, XRPD and N_2 adsorption indicate that POM species have been successfully encapsulated into the MOF without altering its structure. Solid state and solution ³¹P NMR spectroscopy as well as elemental analysis and EDX measurements have evidenced that $[PW_{11}CoO_{39}(H_2O)]^{5-}$ ($PW_{11}Co$) and $[(PW_9O_{34})_2Co_4(H_2O)_2]^{10-}$ ($P_2W_{18}Co_4$) POMs stay intact in the MOF framework. Unexpectedly, the hybrid sandwich-type POMs $[(PW_9O_{34})_2Co_7(OH)_2(H_2O)_4(O_3PC(O)(C_3H_6NH_3)PO_3)_2]^{14-}$ (Co₇-Ale) decompose inside the cavities into $P_2W_{18}Co_4$ anions which are then immobilized. This highlights that one has to be very cautious on the characterizations of the POM@MOF composite materials and that complementary techniques such as NMR spectroscopy, when possible, must be performed to confirm the nature of the encapsulated POM. The two composite materials can be formulated $[Cr_3(H_2O)_3O(O_2CC_6H_4CO_2)_3][PW_{11}O_{39}Co(H_2O)]_{0.2}$ ($PW_{11}Co@MIL$) and $[Cr_3(H_2O)_3O(O_2CC_6H_4CO_2)_3][P_2W_{18}O_{68}Co_4(H_2O)_2]_{0.1}$ ($P_2W_{18}Co_4@MIL$), which correspond to the highest possible loading of POM on the basis of charge balance. This confirms that such negatively charged POMs quantitatively substitute the NO_3^- counter-ions present in the MIL-101(Cr) and that the number of encapsulated POMs thus depends mainly on their charge, providing their size and shape are adapted to the guest material.

Furthermore, the extraction of the POM from the composite POM@MIL materials in 5 M LiCl was analysed by UV-vis, EDX analyses and ³¹P NMR spectra. This indicates that $PW_{11}Co$ can be quantitatively extracted from the MOF while $P_2W_{18}Co_4$ is more tightly bound to the MIL and can only be partly extracted, in agreement with the observation of restricted mobility of the encapsulated POM in $P_2W_{18}Co_4@MIL$ by comparison to $PW_{11}Co@MIL$. Finally, Cl⁻ anions are able to replace the negatively charged POM species, thus confirming again that the interactions between the POM and the MIL are mainly electrostatic.

Further experiments can now be envisioned for $P_2W_{18}Co_4@MIL$ such as magnetic measurements and catalytic water oxidation experiments in order to apprehend the influence of the immobilization of the POM on its properties.

Acknowledgements

Institut Lavoisier de Versailles, UMR 8180, Université de Versailles Saint-Quentin en Yvelines, 45 Avenue des Etats-Unis, 78035 Versailles cedex, France.
*E-mail: catherine.roch@uvsq.fr (C.R.-M.), anne.dolbecq@uvsq.fr (A.D.)*

Electronic Supplementary Information (ESI) available: PXRD (Fig. S1), N_2 adsorption/desorption isotherm and porous distribution (Fig. S2), Table of the specific surface area, total pore volume, and maxima for pore

size distribution (Table S1), EDX analysis (Table S2), UV-vis spectra (Fig. S3-S5), ^{31}P NMR spectra (Fig. S6) and IR spectra (Fig. S7). See DOI: 10.1039/b000000x/

Notes and references

1. (a) J. M.Clemente-Juan, E. Coronado and A. Gaita-Ariño, *Chem. Soc. Rev.*, 2012, **41**, 7464; (b) P. Kögerler, B. Tsukerblat, and A. Müller, *Dalton Trans.*, 2010, **39**, 21; (c) O. Oms, A. Dolbecq and P. Mialane, *Chem. Soc. Rev.*, 2012, **41**, 7497.

2. B. Keita and L. Nadjo, *Electrochemistry of Polyoxometalates*, Encyclopedia of Electrochemistry, Vol. 7 (Eds.: Bard, A. J.; Stratmann, M.), Wiley-VCH, 2006, 607.

3. (a) *J. Mol. Catal. A.*, 2007, **262**, 1-242, special issue on polyoxometalates, ed. C. L. Hill; (b) H. Lv, Y. V. Geletii, C. Zhao, J. W. Vickers, G. Zhu, Z. Luo, J. Song, T. Lian, D. G. Musaev, and C. L. Hill, *Chem. Soc. Rev.*, 2012, **41**, 7572; (c) A. Sartorel, M. Bonchio, S. Campagna, and F. Scandola, *Chem. Soc. Rev.*, 2013, **42**, 2262; (d) J.-F. Lemonnier, S. Duval, S. Floquet, and E. Cadot, *Isr. J. Chem.*, 2011, **51**, 290.

4. (a) B. J. S. Johnson and A. Stein, *Inorg. Chem.*, 2001, **40**, 801; (b) R. Villanneau, A. Marzouk, Y. Wang, A. Ben Djamaa, G. Laugel, A. Proust and F. Launay, *Inorg. Chem.*, 2013, **52**, 2958; (c) S. S. Balula, I. C. S. M. Santos, L. Cunha-Silva, A. P. Carvalho, J. Pires, C. Freire, J. A. S. Cavaleiro, B. de Castro and A. M. V. Cavaleiro, *Catal. Today*, 2013, **203**, 95.

5. Y. Yang, Y. Guo, C. Hu, C. Hu, Y. Wang, and E. Wang, *Appl. Catal. A: General*, 2004, **273**, 201.

6. O. A. Kholdeeva, N. V. Maksimchuk and G. M. Maksimov, *Catal. Today*, 2010, **157**, 107.

7. (a) *Chem. Soc. Rev.*, 2009, **38**, 1201, special issue on Metal Organic Frameworks; b) C. N. R. Rao, A. K. Cheetham, and A. Thirumurugan, *J. Phys.: Condens. Matter.*, 2008, **20**, 083202; (c) G. Ferey, *Chem. Soc. Rev.*, 2008, 37191.

8. J. Juan-Alcañiz, J. Gascon, and F. Kapteijn, *J. Mat. Chem.*, 2012, **22**, 10102.

9. (a) C.-Y. Sun, S.-X. Liu, D.-D. Liang, K.-Z. Shao, Y.-H. Ren, and Z.-M. Su, *J. Am. Chem. Soc.*, 2009, **131**, 1883; (b) J. Song, Z. Luo, D. K. Britt, H. Furukawa, O. M. Yaghi, K. I. Hardcastle, and C. L. Hill, *J. Am. Chem. Soc.*, 2011, **133**, 16839.

10. A. D. Wiersum, E. Soubeyrand-Lenoir, Q. Yang, B. Moulin, V. Guillerm, M. Ben Yahia, S. Bourrelly, A. Vimont, S. Miller, C. Vagner, M. Daturi, G. Clet, C. Serre, G. Maurin, P. L. Llewellyn, *Chem. Asian J.*, **2011**, 6, 3270-3280.

11. S. R. Bajpe, C. E. A. Kirschhock, A. Aerts, E. Breynaert, G. Absillis, T. N. Parac-Vogt, L. Giebeler and J. A. Martens, *Chem. Eur. J.* **2010**, 16, 3926.

12. (a) N. V. Maksimchuk, M. N. Timofeeva, M. S. Melgunov, A. N. Shmakov, Y. A. Chesalov, D. N. Dybtsev, V. P. Fedin and O. A. Kholdeeva, *J. Catal. A*, 2008, **257**, 315; (b) N. V. Maksimchuk, K. A. Kovalenko, S. S. Arzumanov, Y. A. Chesalov, M. S. Melgunov, A. G. Stepanov, V. P. Fedin and O. A. Kholdeeva, *Inorg. Chem.*, 2010, **49**, 2920; (c) A. Micek-Ilnicka and B. Gil, *Dalton Trans.*, 2012, **41**, 12624; (d) L. Bromberg, Y. Diao, H. Wu, S. C. A. Speakman and T. A. Hatton, *Chem. Mater.*, 2012, **24**, 1664; (e) C. M.

13. (a) J. Juan-Alcañiz, E. V. Ramos-Fernandez, U. Lafont, J. Gascon and F. Kapteijn , *J. Catal.*, 2010, **269**, 229; (b) R. Canioni, C. Roch-Marchal, F. Sécheresse, P. Horcajada, C. Serre, M. Hardi-Dan, G. Férey, J.-M. Grenèche, F. Lefebvre, J.-S. Chang, Y.-K. Hwang, O. Lebedev, S. Turner and G. Van Tendeloo, *J. Mat. Chem.*, 2011, **21**, 1226; (c) Y. Zhang, V. Degirmenci, C. Li and E. J. M. Hensen, *ChemSusChem.*, 2011, **4**, 59. (d) J. Juan- Alcañiz, M. G. Goesten, E. V. Ramos-Fernandez, J. Gascon and F. Kapteijn, *New. J. Chem.*, 2012, **36**, 977.

14. I. C. M. S. Santos, S. S. Balula, M. M. Q. Simões, L. Cunha-Silva, M. G. P. M. S. Neves, B. de Castro, A. M. V. Cavaleiro and J. A. S. Cavaleiro, *Catal. Today*, 2013, **203**, 87.

15. C. M. Granadeiro, P. Silva, V. K. Saini, F. A. Almeida Paz, J. Pires, L. Cunha-Silva and S. S. Balula, *Catal. Today*, 2013, **218**, 35.

16. S. S. Balula, C. M. Granadeiro, A. D. S. Barbosa, I. C. M. S. Santos and L. Cunha-Silva *Catal. Today*, 2013, **210**, 142.

17. J. M. Clemente-Juan and E. Coronado, *Coord. Chem. Rev.*, 1999, **193-195**, 361 and references therein.

18. (a) Q. Yin, J. M. Tan, C. Besson, Y. V. Geletii, D. G. Musaev, A. E. Kuznetsov, Z. Luo, K. I. Hardcastle and C. L. Hill, *Science*, 2010, **328**, 342; (b) J. J. Stracke and R. G. Finke, *J. Am. Chem. Soc.*, 2011, **133**, 14872; (c) J. J. Stracke and R. G. Finke, *ACS Catal.*, 2013, **3**, 1209; (d) M. Natali, S. Berardi, A. Sartorel, M. Bonchio, S. Campagna and F. Scandola, *Chem. Commun.*, 2012, **48**, 8808. (e) C. A. Ohlin, S. J. Harley, J. G. McAlpin, R. K. Hocking, B. Q. Mercado, R. L. Johnson, E. M. Villa, M. K. Fidler, M. M. Olmstead, L. Spiccia, R. D. Britt and W. H. Casey, *Chem. Eur. J.* 2011, **17**, 4408.

19. H. El Moll, A. Dolbecq, J. Marrot, G. Rousseau, M. Haouas, F. Taulelle, G. Rogez, W. Wernsdorfer, B. Keita and P. Mialane *Chem. Eur. J.*, 2012, **18**, 3845.

20. R. Canioni, PhD Thesis, 2010, Université de Versailles St Quentin en Yvelines.

21. G. Férey, C. Mellot-Draznieks, C. Serre, F. Millange, J. Dutour, S. Surblé and I. Margiolaki, *Science*, 2005, **309**, 2040.

22. (a) P. Shringarpure, K. Patel and A. Patel, *J. Clust. Sci.*, 2011, **22**, 587-601 ; (b) R. F. Klevtsova, E. N. Yurchenko, L. A. Glinskaya, L. I. Kuznetsova, L. G. Detusheva and T. P. Lazarenko, *Zh. Strukt. Khim.* 1991, **32**, 102.

23. (a) R. G. Finke, M. W. Droege and P. Domaille, *Inorg. Chem.*, 1987, **26**, 3886; (b) T. J. R. Weakley, H. T. Jr. Evans, J. S. Showell, G. F. Tourné and C. M. Tourné, *J. Chem. Soc., Chem. Commun.* 1973.

24. P. M. Paes de Sousa, R. Grazina, A. D. S. Barbosa, B. de Castro, J. J. G. Moura, L. Cunha-Silva and S. S. Balula, *Electrochim. Acta*, 2013, **87**, 853.

25. A. Vimont, J.-M. Goupil, J.-C. Lavalley, M. Daturi, S. Surblé, C. Serre, F. Millange, G. Férey and N. Audebrand, *J. Am. Chem. Soc.*, 2006, **128**, 3218.

26. R. Contant and G. Hervé, *Rev. Inorg. Chem.*, 2003, **22**, 63.
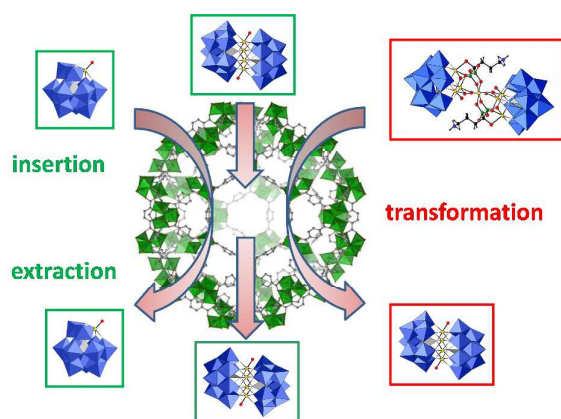
Complementary techniques evidenced the integrity of the monosubstituted and of the sandwich-type polyoxometalates while the hybrid derivative evolves inside the nanocages of the metal organic framework.